HYDRODYNAMIC SHOCK TUBE AND MECHANICS PROBLEMS

V. K. Kedrinskii

Abstract The paper is devoted to some basic experimental and numerical results received under studies of a number of phenomena arising in continued and multi-phase media under shock-wave loading.

Introduction. Some problems of high-velocity hydrodynamics require laboratory simulation of rather strong shock-wave loads with controlled parameters. For these purposes, a variety of hydrodynamic shock tubes (HST) was designed to apply different generation techniques which can be selected depending on specific research objectives. The four basic designs of HST were created: conical (FST), one-diaphragm (GST), electromagnetic (E-MST), and hydrodynamic pulse two-diaphragm tubes (2dST) (Fig.1). These schemes were applied for studying problems in many scientific fields.

Method of high-velocity collision (2dST) [1] was used to determine the velocity and the shift of thermodynamic equilibrium for reversible chemical transformations in solutions and has allowed one to study the relaxation process for the case of temperature and pressure conservation after the jump [2]. The working out of 2dST for generation of strong (up to 1000 MPa) shock waves has required to create the special semi-conductor gauges of pressure [3]. An electric-discharge hydrodynamic shock tubes, wherein a shock wave was produced by an explosion of a wire near the bottom were used for experimental study of the process of shock waves interaction with single bubble, containing passive [4] or reactive gas mixture [5], of its propagations in a two-phase bubble layer. It was shown that of the incident shock wave is splited into two waves : the shock wave pulse (precursor) transformed by the layer and the wave reradiated by a bubble layer [6].

Bubbly media can be considered as the active ones which are able to absorb

[0]Институт гидродинамики им. М. А. Лаврентьева СО РАН, Новосибирск

and to reradiate acoustic pulses and thus to play a role of active media in a problem of "acoustic laser"[7], [8]. The process of excitation of free bubbly cluster (toroidal or spherical clusters) by stationary plane shock waves in HST can be considered as the hydrodynamical analogy of a "pump"in laser systems. Shock tube with sudden changes of profiles in the form of “discontinuities” in cross section was considered as one of the scheme of acoustic laser to study a possibility of SW amplification in the reactive bubble media. The Mach configurations form in the mentioned statements.

The full system of equations for the problem of rarefaction-wave passage over the magma-melt column in the gravity field was derived within the frame work of ST-method. With allowance for diffusion zones and nucleation frequency as a function of supersaturation, the dependence of the number of cavitation nuclei on time formed in the course of phase transformations behind the rarefaction-wave front was found. Let's consider the main schemes of STs (Fig. 1).

I. Shock-tube schemes for shock wave generation

Filler's conical shock tube [9] (Fig. 1*a*) was designed for direct modeling of underwater explosions. The scheme suggests that the parameters of a shock wave generated by explosion of a spherical change in an unbounded liquid can be realized, if a certain spatial angle is separated in the space and a certain portion of the charge is put at its vertex. According this idea, the ideal amplification factor can be determined by the relation of the complete spatial angle 4π to the spatial angle separated by the shock tube cone $2\pi(1-\cos\theta)$ or as $\sin^{-2}(\theta/2)$ and must be equal to 1,070 (for Filler's tube with $2\theta = 7^\circ$). But its actual value turned to be approximately equal to 230: the explosion of a 0.5- g trotyl charge was equivalent to that of a 113-g charge in an unbounded liquid. Finally, the simulation is determined by formula

$$Q \simeq k\frac{q}{\sin^2(\theta/2)}.$$

Here Q is the simulated charge mass, q is the charge mass used in the setup, $k \simeq 0.21$ is the experimental loss coefficient, and 2θ is the full flat angle of the cone.

Glass's one-diaphragm hydrodynamic shock tube [10] is full analogy to the classical gas-dynamic one (Fig. 1, *b*): a diaphragm d separates a high-pressure chamber with gas (G) from a low-pressure chamber filled with a liquid. The pressure behind the SW-front generated in such the hydrodynamic shock tube is obtained combining

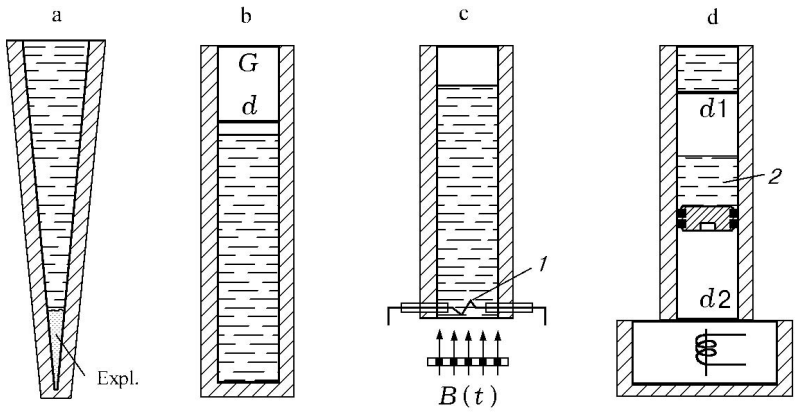

Рис. 1. Schematic diagrams of hydrodynamic shock tubes: *(a)*, Filler's conical tube; *(b)*, Glass's tube; *(c)*, electromagnetic tube; *(d0)*, two-diaphragm tube

the conditions of the parity of mass velocities $u_{sh} = u_2$ and pressures $p_{sh} = p_2$ on the contact discontinuity:

$$\frac{c_l(\gamma-1)}{2c_g}\left\{\left[1-\left(\frac{p_l+B}{p_{sh}+B}\right)^{1/n}\right]\frac{p_{sh}-p_l}{n(p_l+B)}\right\}^{1/2} = 1-\left(\frac{p_{sh}}{p_g}\right)^{(\gamma-1)/2\gamma}$$

The Tait's state equation (Tait's, B=305 MPa, n=7,15 or Ridah's, B=321,4 MPa, n=7, parameters) is using to determine the relations between densities and the speed of sound in liquids. Two interesting conclusions follow from the equation. Firstly, the scheme produces a maximum shock wave amplitude $p_{sh,max}$ in the liquid as an asymptotic value which appears when $p_g \to \infty$ and depends significantly on the type of gas used. Secondly, for relatively weak shock waves generated in a liquid, one can assume that $p_{sh} \simeq \rho_l u c_l$, where u is the mass velocity of the liquid behind the shock wave front. Then, the condition on the contact discontinuity is noticeably simplified

$$\frac{2c_g}{\gamma-1}\left[1-\left(\frac{p_{sh}}{p_g}\right)^{(\gamma-1)/2\gamma}\right] = \frac{p_{sh}}{\rho_l c_l}$$

and after simple transformations is reduced to the form

$$p_{sh}/p_g \simeq 1-\gamma p_g/c_l c_g \rho_l.$$

We can see that the amplitude of the shock wave p_{sh} is practically equal to the initial gas pressure p_g.

Electromagnetic shock tubes [11] are used in two variants, both are based on the same principle of energy storage in a capacitor bank. As a load, the first variant applies either a discharge gap in the working medium or an exploding wire

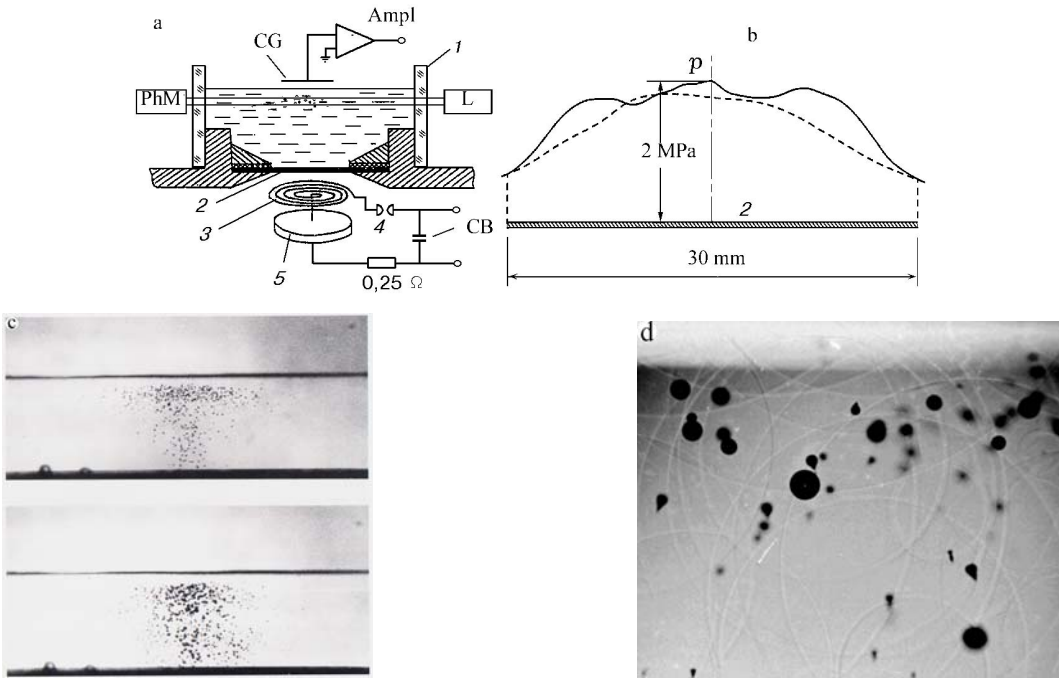

Рис. 2. Schematic diagram of experimental setup (a) for shock wave generation in liquids by magnetic field, wave front profile (b) and cavitation zones (c, 1 μsec exposure time), (d, 3 $nsec$ exposure time)

that stabilizes the discharge channel. In the second case, the bank is loaded on the conductor as a flat spiral coil, wherein pulsed magnetic field is generated by alternating current (Fig. 2,*a*).

Electromagnetic hydrodynamic shock tube designed for generation of ultra-short (microsecond duration) shock waves in a liquid consists of a transparent working section *(1)* 80 mm in diameter filled with distilled water. Central part of the section bottom is a conducting duralumin membrane *(2)* 30 mm in diameter and 0.8 mm thick. The control section of the shock tube (electromagnetic source) is composed of a high-voltage capacitor bank (CB) and a flat spiral coil *(3)* placed between the membrane and the massive copper disc *(5)*. The bank capacity is 2 μF, its inductance is 25 nH. The bank accumulates energy up to 100 J at a voltage of 10 kV. In the discharge chain, the capacitor bank is connected with the spiral by a spark discharge gap *(4)* which operates as a cut-off switch. If the inductance of the discharge chain is low, the "battery — spiral"contour can be closed very rapidly. The contour parameters are adjusted to generate shock waves with amplitudes of the order of 10 MPa, the rise time of about 1 μs, and the duration of 3–4 μs.

Due to diffraction effects the linear dimension of the wave zone generated by the membrane reduces from 30 mm near the membrane to 20 mm near the

free surface of the liquid. It means that a free-wave zone arises in the specimen. Figure 2,*b* presents experimental data for the shock wave front measured by the pressure gauge on PVDF-base in the region under study at distances of 5 (solid line) and 23 mm (dashed line) from the membrane. Fig.2,*c* presents two sequential frames of cavitation zone development between free surface and membrane (1 μsec exposure time). The thin structure of cavitation zone and wave field were resolved using practically instantaneous photograph with 3 $nsec$ exposure time (Fig.2,*d*). Here one can see cavitative bubbles, cumulative jets and a system of shock waves radiated by bubbles. One can note that bubbles in cavitation zone have different sizes and hence they are in different stages of pulsations.

Two-diaphragm hydrodynamic shock tubes allow one to generate shock waves of step type with high amplitudes and durations using the effect of instantaneous deceleration of high-velocity liquid flows on a solid or liquid obstacle. This method was first proposed in [1] and then studied in [12]. Schematic diagram of the setup is shown in Fig. 1,*d*. The shock tube consists of three (or two) sections: high-pressure gas receiver (designed for static pressure up to 20 MPa), acceleration channel with a liquid or solid piston *2* (the channel is partially or completely vacuumed depending in the piston type), and the working section with the liquid separated from the acceleration channel by a diaphragm ($d1$). One can use only two sections, if the liquid under study is used as a piston to generate in it a powerful step like shock wave with amplitude of the order of hundreds of megapascals and duration of the order of hundreds of microseconds.

For measurement of the SW profile at amplitude up to hundreds of megapascals, germanium sensors were used ([1], [3]). The measurement approach was based on a change in the width of the forbidden zone E_G (the width of the energy gap between the filled valent and vacant zones, that is the conducting zone) versus pressure p. Figure 3 shows a typical pressure oscillogram recorded at the butt end of the two-diaphragm shock tube for the impact of a liquid piston on a resting liquid in the working section. The gauge records the first reflected wave *1* with practically constant pressure behind the front. The second jump *2* is a result of the interaction between the waves reflected from the solid part of piston and the tube end. Behind the wave front, there is a pressure decline due to unloading at the lower end of the piston. The third jump *3* is a result of repeated interaction between the waves.

The pressure wave amplitude is calculated from the velocity of the liquid column u during deceleration and from the equation of state (for example, the Tait

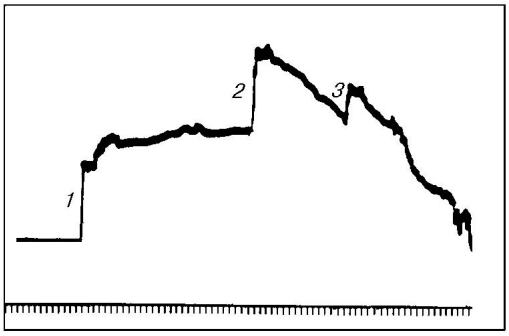

Рис. 3. Pressure oscillogram of shock waves at the butt end of a two-diaphragm shock tube (germanium sensor)

equation)[1]:

$$p_2 - p_0 = \frac{u^2}{4}\Big[\frac{1}{\rho_0} - \frac{1}{\rho}\Big]^{-1}, \qquad \frac{\bar{p}}{\bar{p_0}} = (\frac{\rho}{\rho_0})^n,$$

where ρ and p_2 are the density and pressure in the shock wave front.

II. High-rate reactions in chemical solutions under shock wave loading.

The creation of the two-diaphragm hydrodynamic shock tube [1] is the result of the discussion between Prof. Voevodsky and Dr.Rem Soloukhin (in the beginning of 1960th) on the problem of the working out experimental method of generating strong one-dimensional shock waves of step type in liquid solutions to produce a temperature jump in interval $3 \ldots 30$ °C in a liquid [13] to study the relaxation process for reversible chemical transformations in solutions for the case of temperature conservation after the jump. According to the estimation [14]

$$T - T_0 \simeq 2.6\rho_{sh}p_{sh} \cdot 10^{-2}$$

to realize such temperature jumps you must generate the shock waves with amplitudes in front in interval $10^2 \div 10^3$ MPa. Here T_0 is the initial temperature, in °C; ρ_{sh} is the density, in kg/m^3, and p_{sh} is the pressure behind the shock wave front, in MPa.

Figure 4(I) shows the scheme of an experimental setup: *(1)* pressure gauge; *(5)* condenser; *(6)* diaphragm; *(7)* Jupiter-9 lens; *(8)* light filter; *(10)* conical Plexiglas windows ($d_{min} = 3$ mm, $d_{\max} = 8$ mm, $l = 42$ mm); *(11)* 0.05-mm thick brass membrane; *(12)*, piston. A solution under study *2* was placed in a stainless steel chamber *3*. An incandescent lamp *4* (12 V, 100 Wt) was used as a light source. The shift of equilibrium behind the shock wave front was recorded from the absorption on the appropriate wavelength using a photomultiplier FEU-18A (*9*). Interference light filters *8* or a monochromator PM-2M were used to separate the required wavelength.

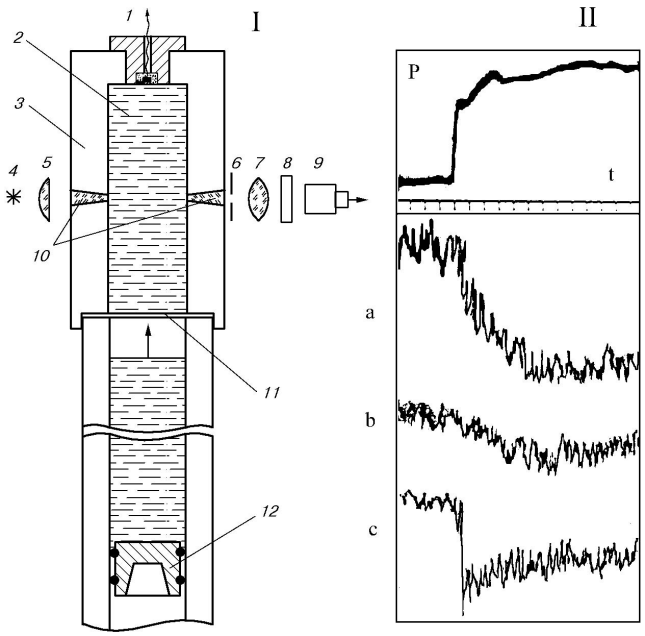

Рис. 4. Schematic diagram of an experimental setup (I) for studying fast reactions and relaxation processes in the fast reactions in solutions (II)

An incident shock wave produced pressure of 110 MPa, the temperature jump was 3 °C, and the heating time of the solution was less than 2 μs.

The efficiency of the technique was tested for two chemical reactions with pronounced temperature effect [13] studied before using other relaxation techniques [15], [16]. As the shock wave passes through an equilibrium solution, the temperature jump behind the front produces an equilibrium shift, which is determined from the change of concentration of the component with the highest absorption factor. The wavelengths that provide maximum light absorption for each reagent were preliminarily measured using a spectrophotometer.

The reaction of tropeolin-0 (weak acid) with water made it possible to test the sensitivity of the method and determine the relaxation time, whose value was compared with that determined in [15]. The shift behind the shock wave front in water solution of tropeolin in neutral medium was experimentally recorded as the tropeolin concentration changed from $0.78 \cdot 10^{-5}$ to $6 \cdot 10^{-5}$ mol/l. The maximum absorption of tropeolin was achieved at 4250 Å.

Experimental results for $T = 22$ °C and the pressure jump amplitude in the shock wave front $\simeq 10^2$ MPa) are shown in Fig. 4(II) (the time scale is 10 μ). Two stages of the relaxation process (II, b) are clearly seen in the oscillogram: an increase in the concentration c after the temperature jump (in about 50 μs the solution has darkened) and then a decrease to a new equilibrium state. The experiments showed that with increasing concentration of tropeolin the relaxation time decreases considerably:τ was changed in the interval $30.5 \div 6.0$.

For tropeolin solved in an alkaline medium, the relaxation process (Fig. 4(II), c), whose character is completely consistent with the experimental data of [15], was observed. The relaxation time constants are close as well. The measurements (at $T = 20^0C$ and $k = 0.714 \cdot 10^{-2}$) showed that the relaxation time constant depends slightly on concentration in the region with low concentration of tropeolin. The constants of electron-transfer rates were measured using the described technique for the reaction

$$\mathrm{Fe}\ (DMBPy)_3^{2+} + \mathrm{Ir\,Cl}_6^{2-} \underset{k_2}{\overset{k_1}{\rightleftharpoons}} \mathrm{Fe}\ (DMBPy)_3^{3+} + \mathrm{Ir\,Cl}_6^{3-}.$$

The complex of bivalent iron has the greatest absorption factor, thus, the equilibrium shift was established on the basis of changing concentration. A typical oscillogram of the relaxation process is shown in Fig. 4(II),a. For equal initial concentrations of reagents $c_0 = 4.35 \cdot 10^{-5}$ mol/l and the ionic force of 0.1 mol, a new equilibrium state has the relaxation time $\tau = 20.7$ μs at $T = 22.1$ °C. The calculated rate constants of direct and reverse reactions (for equilibrium constant $k = 1.95$) are equal to $\sim 8 \cdot 10^8$ and $\sim 4 \cdot 10^8$ l/(mol·s), respectively, and are close to the values obtained in [16]. The above experimental results prove applicability of this technique to studying nonequilibrium processes induced by the temperature jump behind the front of a strong shock wave in solutions.

III. Dynamics of liquid structure in pulsed rarefaction waves

Initial stage. The fracture of a liquid in intense rarefaction waves produced by explosive loading near the free surface is a relatively new field in hydrodynamics of explosive processes. The process involves a series of essentially nonlinear phenomena in the form of successively developing stages of: formation of bubble clusters, unbounded growth of the cavitation bubbles to a foamy structure and disintegration effect. The process can be defined as the inversion of the two-phase state of the medium when the cavitating liquid is transformed into a gas-droplet system. And the HST-method plays important role in the laboratory studies of the mechanisms of the fracture process development corresponding to each its stage.

In contrast to solids, a macroscopic structure of the liquid is such that even when the liquid is carefully purified by distillation or deionization there are always microinhomogeneities, which act as cavitation nuclei. The nature of these microinhomogeneities,

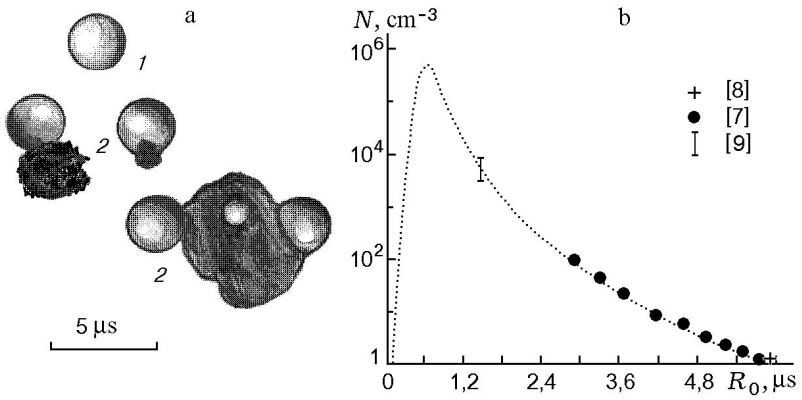

Рис. 5. The structure of microinhomogeneities (a) and the spectrum of cavitation nuclei (b): (1) free gas bubbles and (2) combination structures

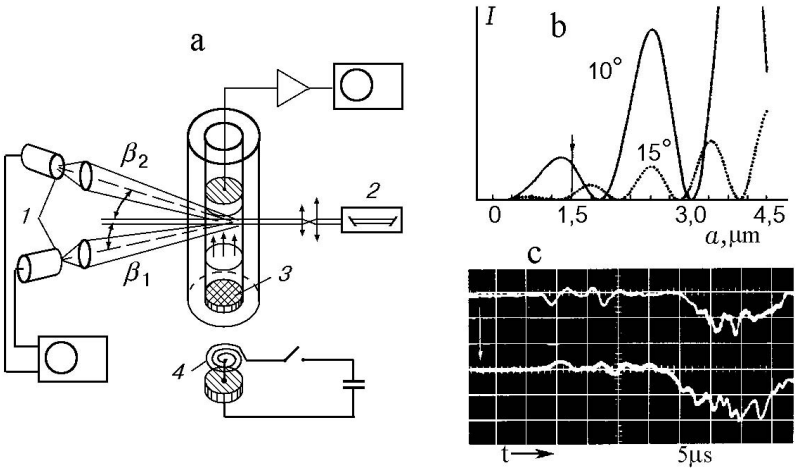

Рис. 6. Electromagnetic shock tube (a), intensity of scattered light versus of the microinhomogeneities size and the viewing angles (b); dynamics of the petals of the scattering indicatrix behind the shock-wave and rarefaction-wave fronts (c); (1) photomultipliers, (2) an He–Ne laser, (3) a membrane, and (4) a plane helical coil in the high-voltage discharging circuit

their parameters, density, and size spectra were studied by a combination of light scattering and electromagnetic shock tube (Fig. 6). The micro inhomogeneities turned out to be microbubbles of free gas, solid particles, or their conglomerates (Fig. 5, *a*).

The liquid sample (distilled water) was placed in the transparent working section of the shock tube (Fig. 6). The light source was a He-Ne laser (a wave length $\lambda = 0.63$ μm) whose beam of diameter 1.5 mm was transmitted at a depth of 3 mm from the free surface of the liquid. The scattered light is collected by photomultipliers whose position relative to the direction of the laser beam was adjusted to the specific features of the problem [11]. Static experiments (unperturbed liquid) with distilled water and show that the radii of the nuclei are approximately 1.5 ± 0.2 μm and their

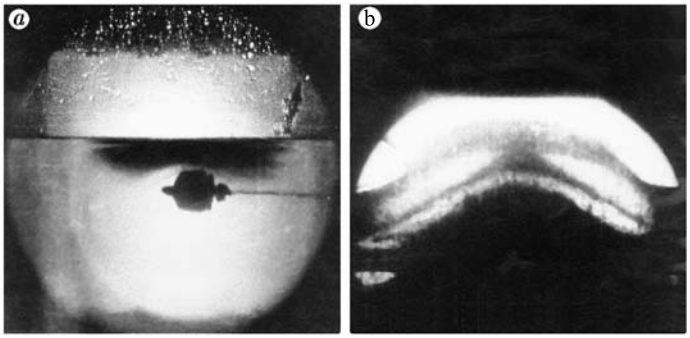

Рис. 7. The cavitation zone under the free surface (a) and two stratified cavitating splits (b) at shallow underwater explosion (early and late stages of the cavitation process, respectively)

distribution is nearly to monodispersed one.

An original technique combining the shock tube and the scattering indicatrix proposed in [11] and based on essential dependence of the intensity of the scattered light on the size of inhomogeneities allowed one to answer on the question concerning the nature of inhomogeneities in a liquid. The distribution of the intensity of the light scattered presented in Fig. 6,b for two observation angles $\beta = 10°$ and $15°$ has shown that the intensity vary in different ways for the selected registration angles (Fig. 6,b): increase with respect to background for $\beta = 10°$ and decrease for $\beta = 15°$ [11]. It is a direct prove of existence of free gas microbubbles among the cavitation nuclei.

Transition to the Fragmentation Stage. Methods of Measurement. As known, for sufficiently intense rarefaction waves bubble cavitation is characterized by unbounded growth of nuclei from the entire theoretically possible size spectrum which can tend to the inversion of two-phase state of medium (to cavitation fracture of liquid). As in the case of underwater explosions near free surface when cavitating splits are developed (Fig. 7) [17]. Short relaxation times of the tensile stress in the cavitation zone as compared with the typical time required for the zone to reach the volume concentration of several dozen percent brought to the conclusion that the process of cavitation fracture has mainly the inertial character. Figure 7,a illustrates one of the initial moments of development of the cavitation zone (dark bow-shaped zone below the horizontal free surface) with adjacent cavity containing detonation products. Later (Fig. 7,b) the cavitation zone disintegrates into several cavitating layers. It means that a cavitating liquid displays brittle properties, which is not characteristic for liquid.

To understand the features of formation and dynamics of the structure of a dense-packed bubble zone (clusters) with volume concentration $0.5 - 0.75$, and the

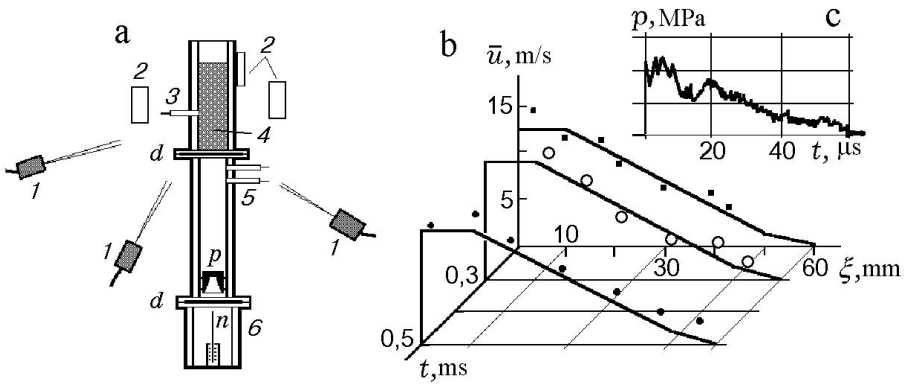

Рис. 8. Shock tube experiments using the x-ray pulse technique (a); the effect of "freezing“ of the mass velocity profile in the cavitating liquid (b); shock wave profile (c): (1) x-ray apparatuses, (2) a photo film, (3) a pressure gauge, (4) a working channel with the liquid, (5) an optical sensor for measuring the piston velocity, (6) a high-pressure chamber

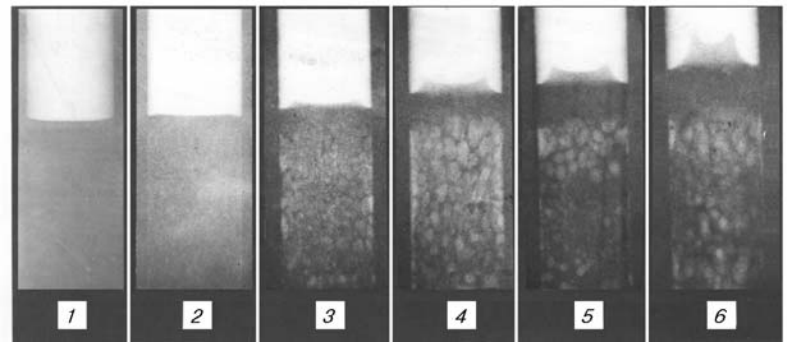

Рис. 9. X-ray images of the dynamics of the cavitation zone (the interval between frames is 200 μs)

transition through the foamy structure to the separation on splits the combination of HST- and pulse x-ray methods was applied.

The cavitation process in intense rarefaction waves was studied using three x-ray devices together with a two-diaphragm hydrodynamic shock tube (Fig. 8,a). The lower diaphragm is ruptured by an electromagnetic system with a needle. The velocity of the piston is measured by fiber-optic sensors 5. High-speed frame-by-frame x-ray recording was provided by synchronization of the starts of each x-ray apparat according to preset time lags (Fig. 9).

The spectrum of the γ-quantum energy of the x-ray devices was adjusted to the resolution of structural inhomogeneities in the few-centimeters-thick layers of a cavitating liquid: the average radiated energy was 70 keV, the maximum energy was up to 200 keV, and the duration of a single burst in the pulse half-height was 80 ns. The amplitude of SW varied within $20 \div 30$ MPa. Fig. 9 shows the x-ray photographs

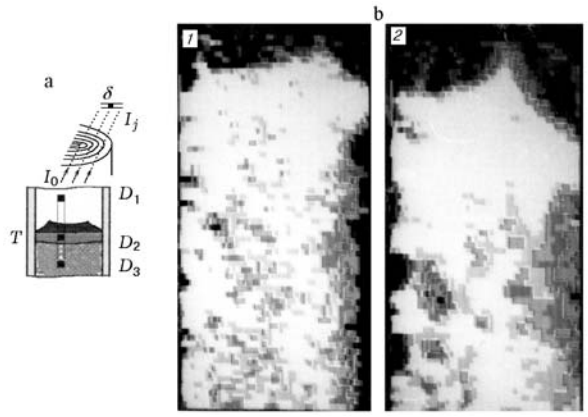

Рис. 10. Constructing a computer analog of the cavitation zone (a); computer version of the x-ray image of at later stage of the process (400 and 800 μs) (b)

for different times from zero to 1 ms. The first frame corresponds to the arrival of the shock wave front to the free surface (the diameter of the free column was 30 mm).

Computer processing of the density distribution of the x-ray negatives enabled the analysis of the structure dynamics without interference by the sensors. Figure 10 shows the method of construction of the computer version based on x-ray photographs (a) [18] and two frames of cavitation zones to the right of the symmetry axis after computer processing and "removing"of the tube wall (b): the density of the dark and light zones corresponds to that of air and the light, respectively. One can see that already after 800 μs there is an intense disintegration of the sample: large voids near the axis and the sample practically separates from the tube wall, near which a dense cavitation zone is observed.

Scanned and computer-processed x-ray negatives of the cavitation zone were used to study the dynamics of the average density $\bar{\rho}$ of the cavitation zone and the time t^* required for the cavitating zone to reach the bulk density of bubbles as a function of the deformation rate of the medium $\dot{\varepsilon}$ [18] (Fig. 11):

$$\bar{\rho} = \rho_0(1 + \dot{\varepsilon}t)^{-1}. \tag{1}$$

One can easily estimate the value of t^* as $t^* \simeq (\dot{\varepsilon})^{-1}$, which is convenient for analysis when the profile and parameters of the shock wave incident on the free surface are known. Following the experimental data, the relaxation time of the medium to the foam-like state for $\dot{\varepsilon} \simeq 1330$ c^{-1} is approximately 700 μs, for $\dot{\varepsilon} \simeq 500$ c^{-1} it is about 2000 μs, which is consistent with the above dependence.

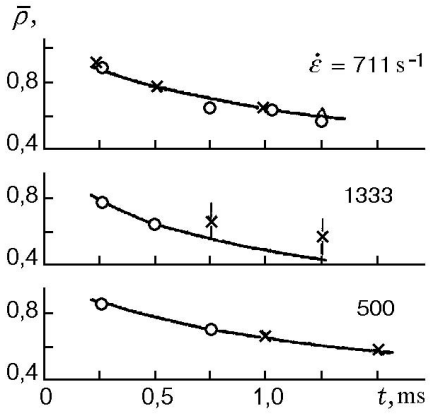

Рис. 11. Dynamics of the mean density of the cavitation zone based on the computer-aided analysis of x-ray photographs

IV. Shock waves in bubble media

In analyzing the behavior of a single bubble in the shock wave field it is usually assumed that the potential ability of bubble to absorb an essential portion of the energy of the incident wave, is insignificant. Thus, it is assumed that the wave field in the liquid surrounding the bubble is independent from the state and dynamics of the bubble. This assumption is not valid for the case of short shock wave interaction with a group of bubbles both due to the finiteness of the energy transferred by the wave over the duration of the interaction and the relatively high energetic abilities of the bubbly area in general. We define short waves as waves whose positive pressure phase is of the same duration as the time of bubble collapse. In the experiments, it corresponds to shock waves with an amplitude of the order of $p_{\max} \simeq 1$ MPa and the positive phase duration of ~ 100 μs for bubble radii of about 3–4 mm.

(I) Shock wave transformation by bubble layer

Under the interaction with shock waves air bubbles are compressed due to the pressure difference in them and at “infinity". As a result, an intense absorption of the energy of the incident shock wave is observed as the wave propagates in the bubbly medium. But simultaneously the oscillating bubble layer reradiates the energy absorbed as secondary wave. The processes occur simultaneously, but their maximum manifestations (the residue of the wave pulse after passing through a bubble layer l and the maximum reradiation of the energy of the incident wave absorbed by the layer) are essentially uncoupled in time [6], [19]. This time interval is a function of the size of bubbles, and it also depends on their concentration in the mixture, the initial parameters of the shock wave, and the layer length. Practically, this time is

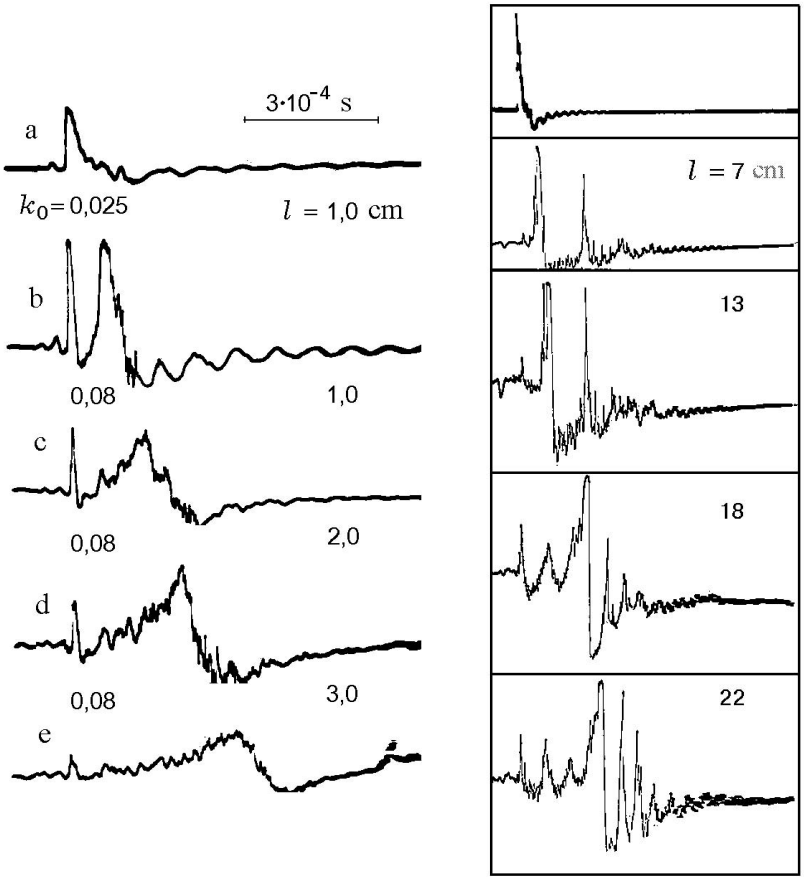

Рис. 12. Splitting of a shock wave into a precursor and a main disturbance for different k_0 and l

Рис. 13. Generation of wave packets by bubble layers for k_0 =0.06 and $l = 0 \div 20$

determined as the time of "collective" oscillation of the bubble layer.

The process of shock wave transformation was studied in detail on an electric-discharge hydrodynamic shock tube, wherein a shock wave was produced by an explosion of a wire near the bottom. Its parameters were changed in the intervals $1 \leq p_{sh} \leq 3$ MPa, and $50 \leq \tau_{sh} \leq 100$ μs.

The passage of shock waves through the bubble medium was studied in detail for a wide range of layer length l and concentration of gas phase k_0: $1 \leq l \leq 30$ cm, $0.004 \leq k_0 \leq 0.3$. Typical pressure oscillograms illustrating in detail the process of the incident shock wave absorption by the layer are shown in Fig. 12 for various values of k_0 and l. The scale of signal amplification at the oscillograms with respect to the shock wave (Fig. 12,a) incident on the layer varied within 2.5 : 1.

Oscillograms in Fig. 12, (b-c) demonstrate the effect of splitting of the incident shock wave (Fig. 12,a) into two waves [6], [19] : a shock wave pulse (precursor) transformed by the layer and a reradiation of the bubble layer ($l = 1$ cm, $k_0 = 0.025$,

$k_0 = 0.08$). The 3rd, 4th, and 5th oscillograms (*b, c*, and *d*, respectively) show the same effect for a fixed concentration of bubbles ($k_0 = 0.08$) but varying layer length ($l = 1, 2$, and 3 cm). One can see that the steepness of the front of the residual shock pulse is preserved practically until it is completely absorbed, while the positive phase is abruptly reduced. The linear dimension of the pulse becomes comparable with the distance between the bubbles. Thus, the medium for this pulse ceases to be "continuous- and now "individual- bubbles not only absorb but also disperse it.

The secondary wave is the reradiation of the incident wave energy absorbed by the layer. The level of "collective- compression of bubbles in layer for the fixed medium and wave parameters will determine the degree of the dissipation of the incident wave energy and the reradiation amplitude, while the inertial character of the collapse process will determine the delay of the onset of the reradiation maximum.

As k_0 or l increases, so does the collapse time of bubbles in the layers, while the radial velocity, the compression degree, and, consequently, the reradiation maximum decrease. It appears that there is such a value $l = l_k$ at which the layer behaves "collectively", it completely absorbs the shock wave energy (the pressure gauges record only a precursor) and reradiates it as attenuating oscillation with their own characteristic frequency.

With further increasing l the process repeats, but now for the wave reradiated by the layer l_k: a new layer l_{k1} arises at which the first reradiation is completely absorbed and reradiated, and instead of it the gauge records a new precursor, etc. The maximum of the second reradiation is determined by the layer parameters and the first reradiation with a delay with respect to its precursor and is recorded with a delay relative to its precursor. The effect of synchronous oscillation of bubbles in the layer is of principal importance, since it not only determines the distinct structure of the reradiated compression wave but also indicates the ability of the bubble system to "independent generation- of peculiar coherent structures in the medium.

Figure 13 shows the oscillograms of the wave field under the interaction of the shock wave with bubble layer (up to 22 cm long) for volumetric concentrations of the gas phase $k_0 = 0.06$ One can easily notice the following. Firstly, the wave energy is absorbed immediately behind the front, it changes the amplitude and the duration of the pulse and "splits- it but does not change the front steepness. Secondly, the "split- pulse retains its position in time, while the maximum of the wave reradiated by the medium shifts to the right in the oscillograms (see the top-down sequence). The character of the reradiation suggests synchronous collapse of bubbles, i. e., the

layer behaves as a coherent structure. The experimental data confirm the existence of a series of precursors and indicate the distinct periodic structure of the resulting signal. Thirdly, the length of the coherent layer l_k is limited and is determined for each concentration and initial parameters of the shock wave.

(II) SASER: Shock Amplification by Systems with Energy Release

It was shown in [20], [21], [22] that both cavitating and bubble systems with a nonreactive gas phase and explosive gas mixtures can be regarded as reactive media capable of absorbing external disturbance energy, amplifying the disturbance, and then reradiating it as a power acoustic pulse. Studies of these systems in designing hydroacoustic analogs of laser systems (hydroacoustic "lasers- or SASER [22]) involve the problem on the transmission of an acoustic pulse generated by the system into a liquid with the least losses.

(II.I) Shock tube with changing cross sections. Effect of bubbly detonation

Statement of the Problem. Shock tubes with sudden changes of the cross section area and a one-phase liquid waveguide can be considered as one of approaches to solution of SASER problem (Fig. 14) [22]. Sudden changes in the cross section area of a shock tube of radius R_{ST} (Fig. 14) are produced by changes in shock-tube profile (transition from section 1 to section 2) or/and by inserting a coaxial rigid cylinder (radius r_{cyl} and length L_{cyl}) forming an annular channel 1 filled with a two-phase mixture similarly to section (2). The condition $L_{\mathrm{SW}} \leq L_{\mathrm{cyl}}$ is satisfied. Here L_{SW} is the characteristic distance at which the steady-wave regime of bubbly detonation initiated at the left butt end of the shock tube is established. The inner geometry of the channel stimulates the wave reflection and focusing (the pressure in region 2 is modified by varying the distance L between the butt end and the wall) in the bubbly medium as the acoustic pulse generated by the waveguide 3 (radius r_{out}) intensifies.

Two-Phase Model. To describe wave processes in bubbly hydrodynamic shock tubes the physico-mathematical model based on the modified IKvW model [23], [24], [25], [26], [27], [28] is used. For a reacting gas phase the model is supplemented by

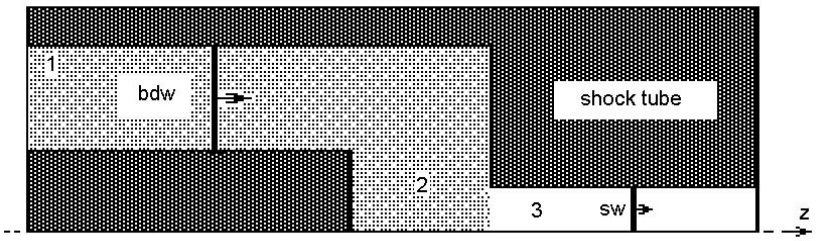

Рис. 14. Shock tube channel geometry with sudden expansion and contraction of the channel: (1) annular channel; (2) working section; (3) waveguide.

the equations for kinetics of chemical reactions: by the Todes kinetics [29], by general kinetics [30] or by simple condition of instantaneous adiabatic explosion at constant volume [28]. Analysis of different approaches to the description of wave processes in reactive media containing bubbles filled with explosive gas mixtures shows that it suffices to restrict oneself by the frames of the above simplified statement [28].

This statement suggests that when gas in bubbles is heated to the ignition temperature the reaction occurs instantaneously after the appropriate degree of compression of bubbles (R_0/R^*) is achieved. An adiabatic explosion occurs, the bubble volume remains unchanged, and the pressure p_g in the bubble increases instantaneously to $p_* = \rho_*(\gamma_* - 1)Q_{\text{expl}}$ (Q_{expl} is the explosion heat and ρ_* is the density of the detonation products). The adiabatic exponent becomes equal to that of detonation products γ_*. Thereafter the process develops under new "initial-conditions without a change of the mathematical model.

In the calculations for the case of a reactive bubbly medium the gas mixture $2H_2+O_2$ was considered. At the time t =0 a constant pressure $p(0)$ is specified on the left boundary of the shock tube. The numerical scheme was tested by the example of the one-dimensional problem on the formation of wave structures in the shock tube of constant cross section filled with a liquid containing gas bubbles. Characteristic structures of steady shock waves in the nonreactive and reactive media are presented in Figs. 15,a,b respectively, horizontal dotted lines mark the values of pressure jumps $p(0) = 1.0$ MPa specified at the tube butt end and initiating the wave process. In both cases the gas-phase volume fraction was $k_0 = 0.01$ and the bubbles were of the same size ($R_0 = 0.1$ cm). For the indicated parameters, the establishment of a steady-state regime, for example, for a bubble detonation wave (with the maximum amplitude of about 15.0 MPa), is recorded at a distance of $x \approx 15$ cm from the left wall of the shock tube. Quasi-stationary wave regime in the bubbly medium with a chemically active gas phase was discovered in the result of experimental studies of

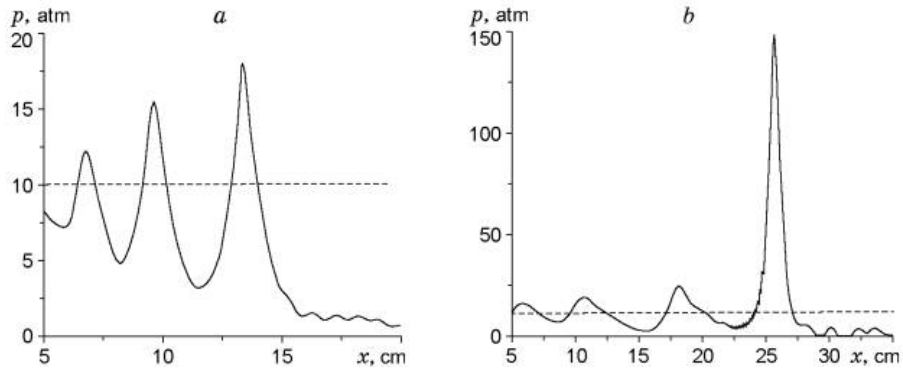

Рис. 15. Characteristic profiles of steady shock waves in nonreactive (a) and reactive (b) media

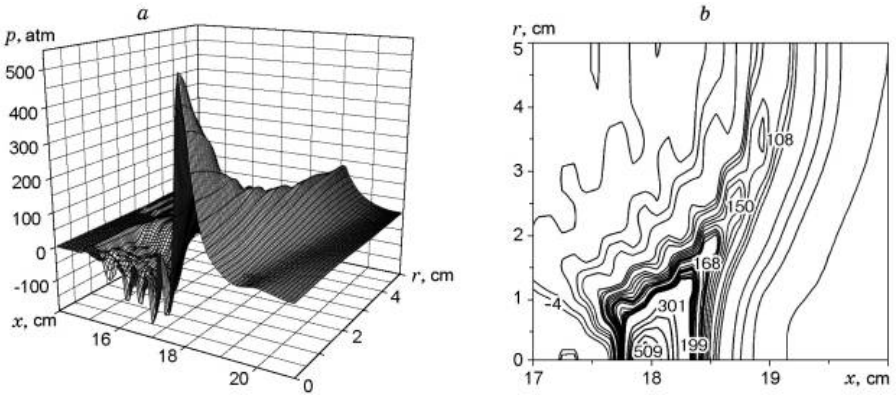

Рис. 16. Focusing of bubble detonation wave (a) and Mach disc structure

SW in hydrodynamic shock tubes [31], [32] and it was called by bubbly detonation wave.

Expansion, Focusing and Reflection of a Bubbly Detonation Wave. It is obvious that as the wave comes out of the circular channel 1 (Fig. 14) in the section 2 a few effects can be observed. Firstly, a rarefaction wave arises behind the rod edge. But the energy radiated by exploding bubbles compensates for the wave losses and the wave can be amplified due to the focusing (Fig. 16,a).

Secondly, as follows from Fig. 16,b at a certain distance from the rod edge the wave reflection from the axis becomes irregular. In the reactive bubbly medium ($k_0 = 0.01$, $R_0 = 0.1\ cm$) a Mach disc is formed, whose characteristic width is over 1 cm for a relatively small focusing radius $r_{cyl}/R_{ST} = \ 0.5\ cm$ [33]. The Mach disk has a core with high pressure in the center and rather abrupt pressure gradient to the periphery. The core is limited by the system of closed isobars. Thirdly, the detonation wave having in the vicinity of a tube wall an axisymmetrical "nature"reflects from a solid wall with a hole, which is a waveguide outfall. Analysis of the calculation

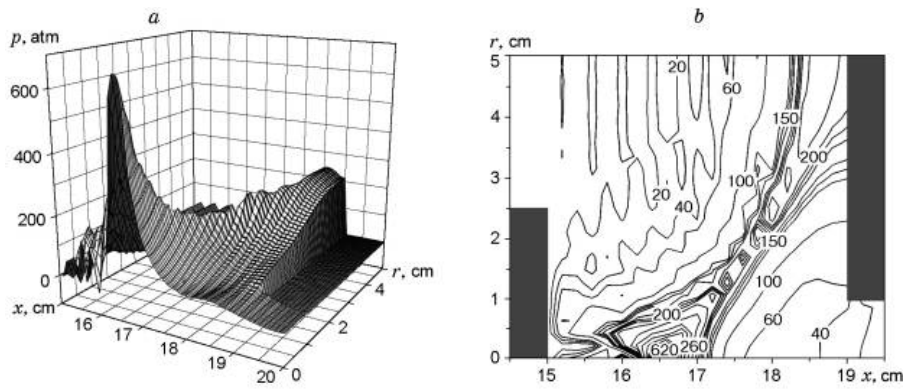

Рис. 17. Wave field structure in the channel 2, focusing of the wave reflected from the wall

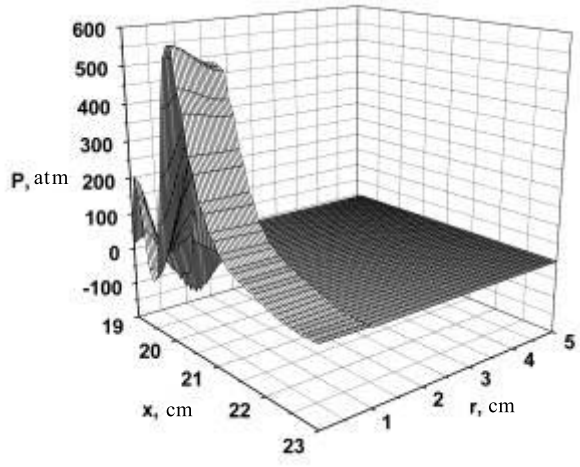

Рис. 18. Solitary shock wave in the waveguide

results for the wave field shows that the bubble detonation wave reflected from the wall has a spatial circular form and is focused too on the symmetry axis of the shock tube (Fig. 17) [33].

Calculations show that in a general statement one can use both focusing effect for the amplification of the wave radiated in the waveguide, for example, by selecting the parameter L (the distance between the rod edge and the wall with hole). Thus, the Mach configuration can be formed in the vicinity of the contact boundary. As the second governing parameter one can use the waveguide radius r_{out}, whose value should be adjusted to the Mach disc, so that practically a one-dimensional configuration of the wave field is formed in the waveguide channel. For example, if the waveguide radius is equal to the rod radius $r_{out} = rcyl = 2.5\ cm,\ r_{cyl}/R_{ST} = 0.5$), the pulse amplitude in the waveguide is 200 atm. As the waveguide radius r_{out} decreases to the size of the Mach stem (about 1 cm), the wave amplitude increases to 500 atm (Fig. 18) [33].

(II.II) Shock Tubes with Free Bubbly Systems.

Often so-called problems of hydroacoustic analogies of "laser"systemsthese problems are not limited by the requirements of energy cumulation, but involve the problem of directional radiation. The active media capable of absorbing the external disturbance, amplify and reradiate it as an acoustic pulse is also one of the important element these systems. Since the “free- systems may be of principal importance for experimental studies, we consider the statements focused on analysis of the interaction of shock waves with bubble clusters. The wave processes in such free systems are distinguished by a wide spectrum of time and space parameters, associated with the generation of shock waves with the amplitudes of tens of megapascals, and governed by a great number of parameters whose effect can hardly be analyzed in physical experiments.

Therefore, the dynamics of the state of complicated active systems and the development of wave processes in them are simulated numerically. The numerical analysis of the interaction of a plane stationary shock wave with a nonreactive clusters within the framework of a two-phase mathematical model of a bubbly liquid shows that the difference in the wave propagation velocities in the cluster and the ambient liquid, as well as the selection of a real cluster geometry, lead to unexpected effects, which will be analyzed below.

Toroidal bubble cloud, Mach disks

Statement of the problem. At a moment $t = 0$ a piston generates a pressure jump at the butt end of a cylindrical shock tube of radius r_{st} filled with water. The shock tube contains a toroidal bubble cluster, whose center is placed on the z-axis of the shock tube at a distance l_{cl} from its left boundary. The plane of the base circle of the tore (further the torus plane) of radius R_{tor} ($R_{tor} < r_{st}$) is perpendicular to the shock tube axis, the torus section radius is R_{circ} (Fig. 19).

The volumetric concentration of the gas phase in the cluster is k_0. Gas bubbles at the initial moment of time have the same radius R_b and are uniformly distributed in the toroidal cluster. At $t > 0$ the external shock wave propagating along the positive z-axis interacts with the toroidal bubble cloud, envelops it, and refracts into the cluster in the zone of contact with the front. The refracted wave propagates inside the cluster and is transformed by the bubble system. The difference in the

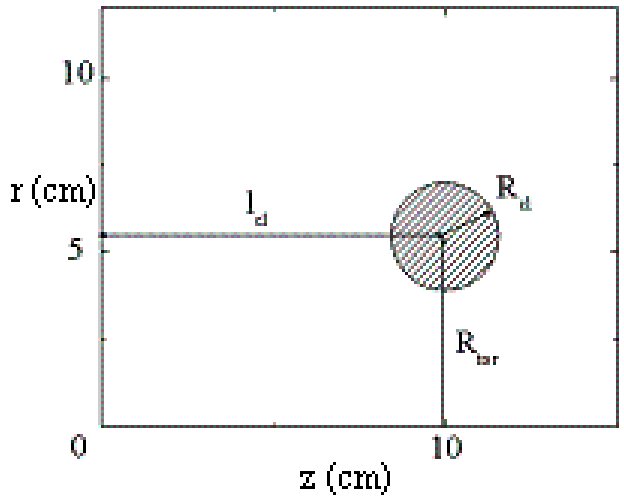

Рис. 19. Layout of a toroidal bubble cluster (the torus radius is hatched, z is the symmetry axis)

propagation velocities of the external shock wave in the liquid (1.5 km/s) and in the bubbly medium (hundreds of meters per second) leads to the formation of a shock wave with a concave front inside the torus. The focusing results in the amplification of the wave inside the cluster to the level governed by the system parameters and the radius of the torus section R_{circ}. The shock wave amplified by the cluster is radiated in the ambient liquid as a toroidal quasi-stationary shock wave with oscillating profile. The transformation and focusing of the refracted wave in the cluster were calculated using the modified IKvanW model [34], which represents a physically heterogeneous medium as a uniform medium with peculiar properties described by the Rayleigh equation.

Dynamics of wave field structure. A typical pattern of isobars for different times of focusing of a shock wave generated by a toroidal bubble cloud is shown in Fig. 20 (a-c). The value of pressure can be estimated from the scale of distribution of the relative pressure p (in the units of hydrostatic pressure $p_0 = 0.1$ MPa). Each moment is presented by two photos: a general view (on the right) and a close-up (on the left) of the region limited by the torus plane $z = 10$ cm, its radius R_{tor}, and the front of the shock wave interacting with the torus (in the right photos). The calculations were performed for the following parameters: p_{sh}=3 MPa, r_{st}= 20 cm, z_{max}=40 cm, l_{cl}=10 cm, R_{tor}=6 cm, R_{circ}=1 cm, k_0 =0.01, and R_b=0.1 cm.

Figure 20,a shows the wave field before axial focusing of a shock wave radiated by the torus. The axial reflection of the toroidal wave becomes irregular already at the initial stage (Fig. 20,b), which is clearly demonstrated by the form of the first isobar of the incident wave. In the same photo, there is the second maximum of the

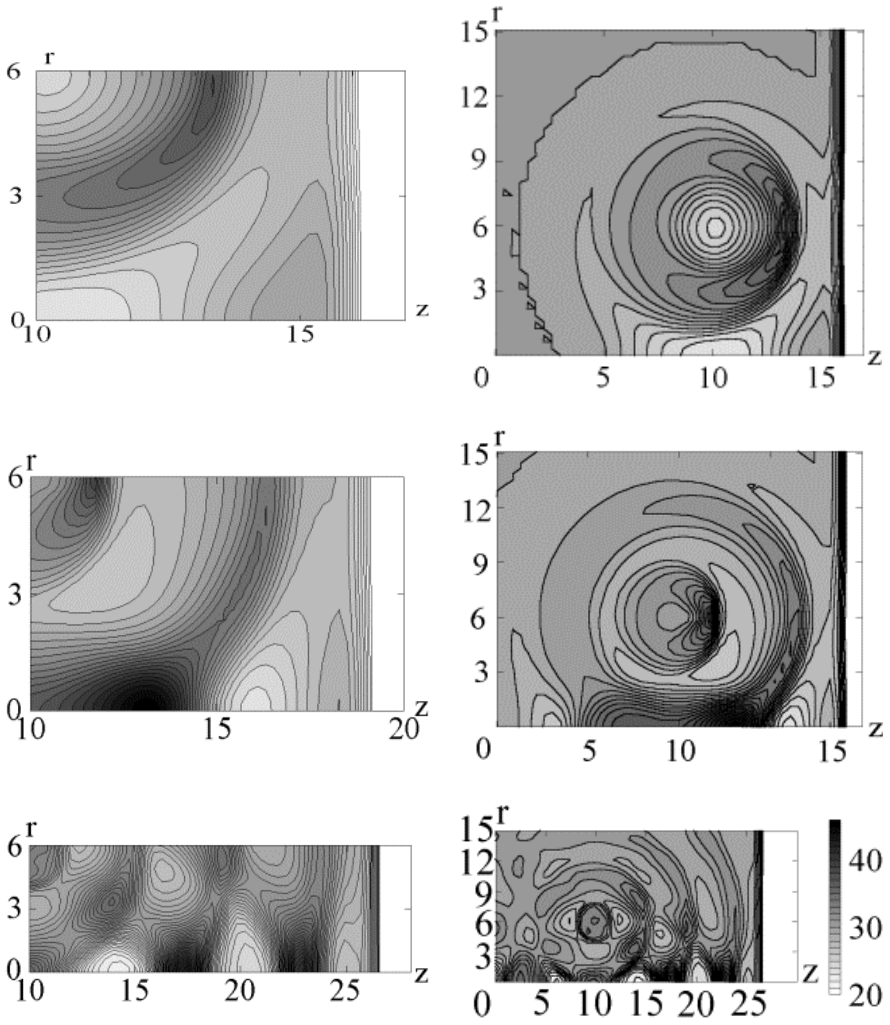

Рис. 20. Pressure fields as a system of isobars presented for the times $t = 110$ μs (a), $t = 130$ μs (b), and $t = 180$ μs (c) (two shots for each, the reflection zone scale is magnified in the left shots)

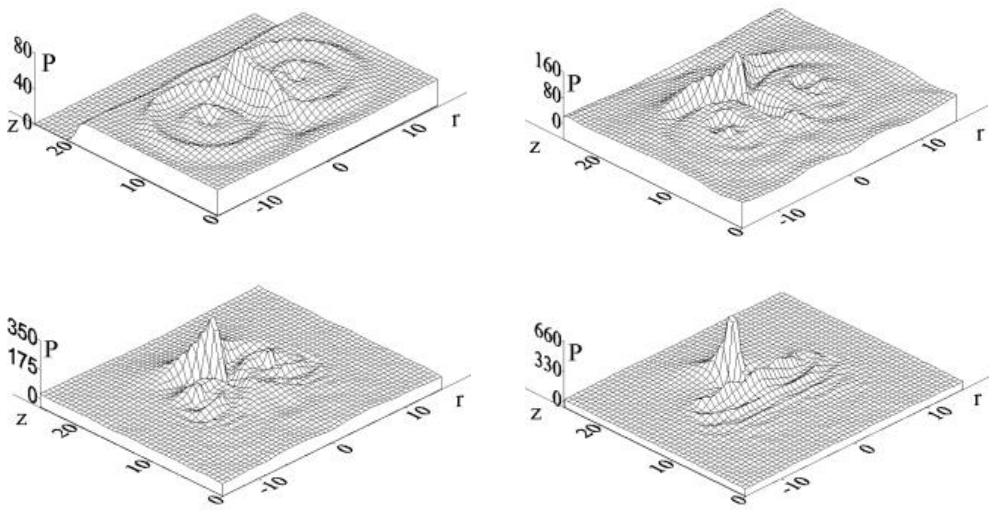

Рис. 21. The radius of the section of a bubble torus vs. the evolution of the first solitary wave generated by the torus in the liquid: (a) R_{circ} = 0.5 cm, (b) R_{circ} = 2 cm, (c) R_{circ} = 4 cm, (d) R_{circ} = 6 cm.

oscillating shock wave generated by the cluster. The third pair of photos (Fig. 20,c) demonstrates the formation of two Mach discs on the axis [34]. The width of the zone of axisymmetrical irregular reflection (the Mach disc) turned out to be finite and equal to 4-5 cm. A high-pressure zone limited by the system of closed isobars, which can be defined as the Mach disc core.

At first sight the unexpected effects arise as one of the geometrical parameters of the torus, the radius of its section R_{circ}, changes at fixed radius of the base circle R_{tor} (Fig. 21, a-d). The results are presented for R_{circ}=0.5, 2, 4, and 6 cm at fixed p_{sh}=3 MPa, R_{tor}=6 cm, k_0 =0.01, and R_b=0.1 cm. The flow topology remains practically unchanged for the first three values of R_{circ}. Calculations show that with increasing R_{circ} there is a considerable increase of the wave amplitude in the Mach disc core: p =81.7 at R_{circ}=0.5 cm, p =99.4 at R_{circ}=1 cm, p =166 at R_{circ}=2 cm, p =258 at R_{circ}=3 cm, p =386 at R_{circ}=4 cm, p =568 at R_{circ}=5 cm, and p =859 at R_{circ}=6 cm.

In the fourth case, R_{circ}= 6 cm, the inter torus boundary closes in a point on the axis and the dynamics of the pressure field in the liquid modifies considerably. The flow cumulation finally leads to the formation of a strong solitary wave in the near zone with the amplitude exceeding that of the wave interacting with the torus by almost a factor of 30 (Fig. 21,d) [34].

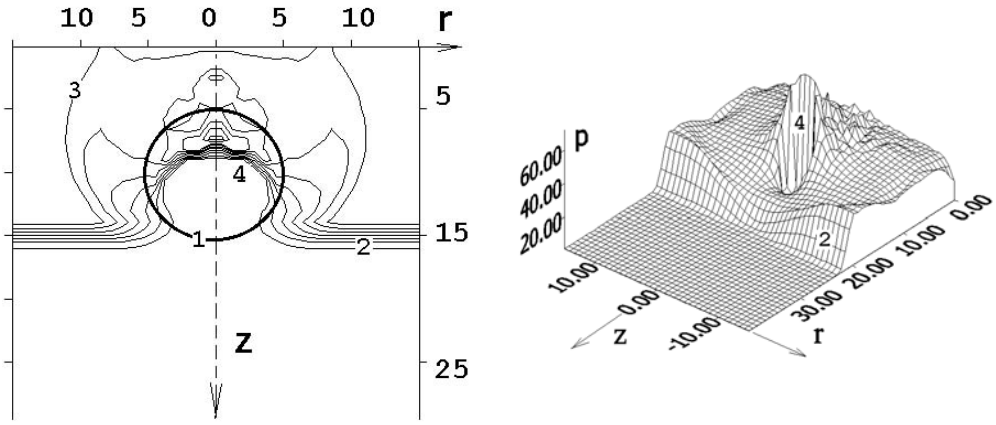

Рис. 22. The interaction of a shock wave with a bubble cluster and the pressure distribution $p(r,z)$ for t=140 μs

Spherical bubbly clusters: SW cumulation with a pressure gradient along front

Statement of the problem is the same as the above mentioned. A shock wave generated at a time $t = 0$ at the butt end of a cylindrical shock tube propagates along the positive z-axis and collides with a spherical bubble cloud of radius R_{cl} with the volumetric concentration of the gas phase k_0. A center of a spherical bubble cluster is placed on the z-axis of the tube. Gas bubbles in the cluster have the same initial radius R_0. An incident shock wave envelops a cluster and excites with a delay in different points of its surface an internal shock wave. The shock wave is formed in the cluster in a result of the reradiation of the refracted wave absorbed by bubbles.

Calculation results. Figure 22 presents the schemes of interaction of a bubble cluster (1 is the cluster boundary) with a shock wave (2 is the incident shock wave front, 3 is the system of isobars,(4) is the shock wave front in the cluster) for the time $t = 110\ \mu s$. The calculation was performed for the amplitude of an incident shock wave $p_{sh} = 3\ MPa$, $k_0 = 0.01$, $R_0 = 0.1\ cm$, $R_{cl} = 4.5\ cm$, $l_{cl} = 10\ cm$ (for tube radius $r_{st} = 15\ cm$). Calculations (Fig. 22, $p(r,z)$) prove that, although by 110 μs the front of the incident wave 2 completes enveloping the cluster, a part of the bubbly zone (restricted by the curvilinear front of the wave generated by bubbles remains unperturbed. By the time $t = 140\ \mu s$ the initial stage of the wave amplification is observed (see Fig. 22): the focusing zone in the cluster is formed, one can distinctly see the pressure gradient along the curvilinear front 4 in the bubbly system. The focusing leads to the formation of a strong shock wave with the amplitude p_{foc} of

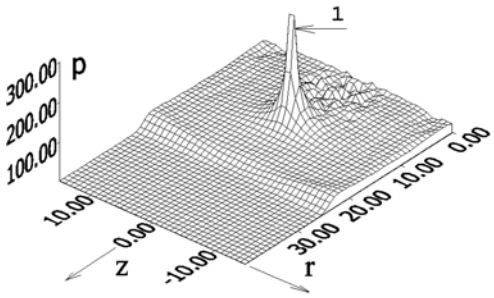

Рис. 23. Generation of a strong acoustic pulse 1 by a cluster ($t = 160\ \mu s$)

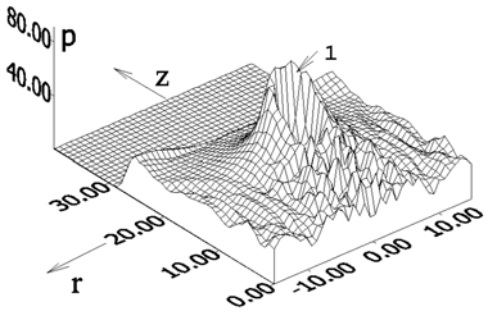

Рис. 24. Profile of the shock wave 1 radiated into the liquid by a bubbly cluster (t=180 μs)

over 30 MPa (Fig. 23, $t = 160\ \mu s$) at the cluster-liquid interface near the coordinate. Then, the cluster generates a shock wave in the ambient liquid. The wave 1 is of the "bore- type (Fig. 24) with the front envelope as a parabola, a pressure maximum on the axis, and rather abrupt decline along the "branches"($t = 180\ \mu s$) [27].

It is necessary to mention the "nonclassical" type of the focusing accompanied by the absorption of the shock wave in the cluster by gas bubbles and their subsequent reradiation.

Regarding the production principles for the sources of a strong acoustic pulse, one can conclude that the nonreactive bubble clusters excited by the shock wave are an active medium capable of absorbing, amplifying, and reradiating the external disturbance as a strong acoustic signal [27]. To control the location of the focus field with respect to the "spherical cluster-liquid"interface and, consequently, to eliminate the absorption of the cluster-generated bubble by the cluster, one should properly select the volumetric concentration of the gas phase k_0.

V. Shock-tube methods in the problem of simulation of explosive eruption of volcanos.

Researches of processes of explosive volcanic eruption are directed basically on studying silicon magma state at sudden decompression, its fragmentization and the initial stage of explosive eruption characterized by kinetics of formation of cavitation nuclei and crystallization [35].

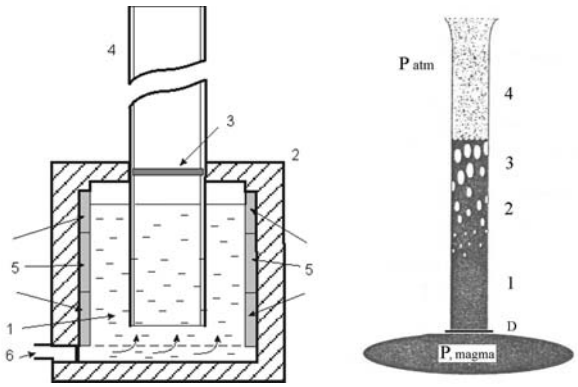

a) b)

Рис. 25. A chamber - thermostat of a high pressure (a) and circuit F.Dobran (b).

In [36] it is marked, that statements of laboratory experiments with shock tubes (ST) on modeling dynamics of volcanic streams are important components of researches. During many years a basic attention is given to mechanism of cavitative destruction of magma: transition of system from cavitative state to gas-droplet one. Note, that these problems were earlier considered in detail for samples of distilled water (see [37]). But in spite of numerous experimental and theoretical studies at present the detailed dynamics of decomposition of liquid magma (with complex kinetics of transitions) practically is still far from understanding. Here we will mention only some results connected with the features of dynamics of flow structure which is developed in preliminary compressed magma under decompression wave. We mean the simulation of initial stage of volcano eruption and the attempts to understand the influence of permanent and dynamically changing viscosity of medium on its flow structure.

The experimental research of influence of viscosity of hydrodynamic analogues of magma (M–liquids) on structure of flow was carried out using the hydrodynamic shock tube method (fig. 1, a, b) with a researched liquid 1 in the chamber of a high pressure 2 separated by the valve 3 from working channel 4 with atmospheric pressure. Through input 6 under pressure in 0.5 MPa the liquid 1 was saturated with carbonic gas. The liquid has being pushed out in the channel 4 by gas pressure above its free surface at opening the valve. In a result of sharp pressure drop the process of M-liquid nucleation and its structure dynamics at eruption could be investigated. Set up included the scheme of optical registration of the processes, consisting of system of delays for the pulse light source with an exposition about 1 microsecond, allowing to receive the instant photo of flow structure for the various moments of time and then to build a frame-scanning of fracture process.

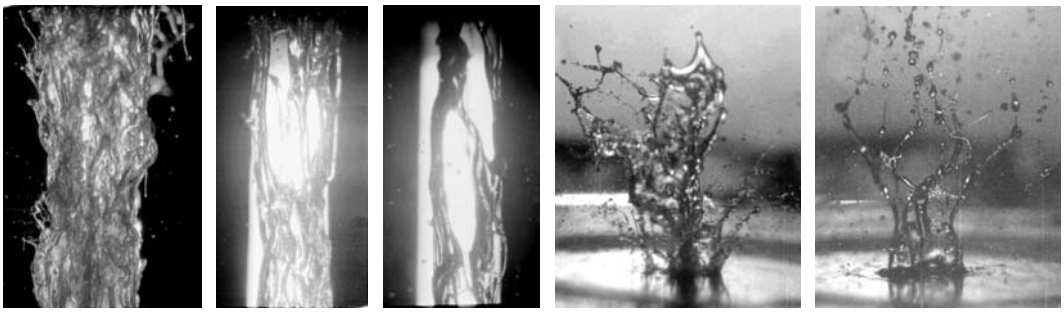

a) b) c)

Рис. 26. Foamy structure of a stream (a) and his stratification on a jet (b, c)

a) b)

Рис. 27. Jet structure of flow at shock-wave fragmentation of gum rosin - acetone drop

Installation allowed one to check the eruption model (fig. 1, b) suggested in [38] according to which in a result of destruction of a fuse (diaphragm D) a magma under unloading begins to move upwards along the channel. It was assumed that a few zones of states are formed in a stream. The stream remains homogeneous (1) only in the vicinity of a mouth of the channel, further upwards on a stream the nucleation and formation of cavitation zones (2) are observed. The latter in a result of diffusion of water vapors (dissolved in magma) in bubbles is transformed to structure like a foam (3). Further it is supposed, that as a result of destruction of foam the process of inversion of a two-phase state - transition from cavitating liquid to a state of type gas-suspensions (4) should be realized. We can conclude that there is full analogy to effects of cavitation development and liquid disintegration (Fig.7) under shock wave loading considered above.

Fig.2,a-c presents the characteristic dynamics of eruption structure for two types of viscous liquids in the vicinity of output from the channel: the increased scale of a site of liquid stream with viscosity 0.2 Pa·sec ($T = 19°$C, fig. 2a), structure of the same site after some time interval (fig. 2b) and the structure of liquid stream with viscosity 2.6 Pa·sec, $T = 42°$C (fig. 2c) with the same resolution and for the same site. Apparently, the resolution of fine structure of stream, due to increase in scale and a microsecond exposition, allows one to find out its essential change: effect of flow stratification on a system of vertical jets having a spatial form (fig. 2 b, c). At increase in viscosity the stream gets more precise jet character (fig. 2c). The probable reason of this effect has been found out at research of various stages of eruption of various viscosity liquids saturated with gas. Appeared, that in various zones of cavitating stream in result of bubble coalescence the gas slugs (fig. 3) are

spontaneously formed. The combinational structure of such stream during the time is transformed in a stratified jet flow, characteristic for all studied range of viscosities. These results show, that the mechanics of destruction of a stream has more complex character, than was described above [38], [39].

Note, the method of shock tubes (ST) enables in a dynamic regime (in real time scale), using system consecutive loading "shock wave — rarefaction (unloading) wave" to model process sudden decompression of a magma which before eruption is in a statically compressed (up to high pressure) state. Besides the method of electromagnetic ST allows one to generate in a studied sample short, microsecond duration shock waves and, thus, to use very small liquid samples, for example as drops about 1 cm in diameter, for more precision research of flow structure.

Experiments on dynamic loading of water drops by shock waves (SW) have shown, that change of their structure consists in the formation of system of bubble clusters on surface and inside of drop. Fast expansion of clusters and bubble coalescence in them result in effect of internal cavitative explosion of a drop and its transformation in system of cells formed by liquid "cords".

Besides as M-liquid we studied the "gum resin-acetone" solution which even at room temperature has one of the important property characteristic for magma – it can be crystallized and dynamically change of viscosity under fast decompression. The last is achieved due to evaporation of acetone in rarefaction wave. Hence fast crystallization of a solution can be observed during its dynamic destruction. As the experiments showed the destruction of such solution drop completely differs from picture mentioned above (fig 3). Instead of the dome-shaped form with cellular structure characteristic for the last stage of water drop disintegration the system of vertical jets (fig. 3a, instant of time 2 ms) is developed and then it's disintegrated due to instability on smallest droplets (fig. 3b, 5 ms).

Work was carried out under financial support of Russian Foundation of Basic Research (grant 03-01-00274), Leading Scientific School (grant SS-2073-2003.1) and Integration Project 1C SB RAS.

СПИСОК ЛИТЕРАТУРЫ

1. *Vorotnikova M.I., Kedrinskii V.K.., Soloukhin R.I.* (1965) Shock tube for study of 1D waves in liquid. // Combustion, Explosion and Shock Waves, №1. p.5-15

2. *Kedrinskii V.K., Serdyuk N.K., Soloukhin R.I., Stebnovsky S.V.* (1969) Study of fast reaction in the solution behind of front of strong shock wave. // Doklady of the USSR Academy of Sciences, v.187, №1, p.130-133

3. *Kedrinskii V.K.., Soloukhin R.I., Stebnovskii S.V.* (1969) Semi-conductor pressure gauge for measurement of strong shock waves in liquid ($> 10^3$ atm).// J of Applied Mechanics and Technical Physics, №4, p.92-94

4. *Kedrinskii V.K., Soloukhin R.I.* (1961) Compression of spherical cavity in a water by shock wave. // J of Applied Mechanics and Technical Physics, №1, p.27-29

5. *Soloukhin R.I.* (1960) About bubble mechanism of shock combustion in liquid.// Doklady of the USSR Academy of Sciences, v.136, №2, p.311-312

6. *Kedrinskii V.K.* (1968) Disturbance propagation in a liquid with gas bubbles. //J of Applied Mechanics and Technical Physics, №4, p.29-34

7. *Volkov I.V., Zavtrak S.T., Kuten I.S.* (1997) // Rev. E., v.56, n.1, p.1097-1101

8. *Zavtrak S.T., Volkov I.V.* (1997) // JASA, v.102, n.1, p.204-206

9. *Filler W.S.* (1964) // Phys. Fluids **7**, 5

10. *Glass I.I., Heuckroth L.E.* (1963)// Phys. Fluids **6**, 4

11. *Besov A.S., Kedrinskii V.K., Palchikov E.I.* (1984) //Pis'ma Zh. Exp. Teor. Fiz. **10**, 4

12. *Kheiman F.* (1968) // Theor. Fundamentals of Eng. Calc. **90**, 3

13. *Kedrinskii V.K., Serdyuk N.K., Soloukhin R.I., Stebnovskii S.V.* (1969)// Dokl. Akad. Nauk SSSR **187**, 1

14. *Kuznetsov N.M.* (1961) //Zh. Prikl. Mekh. i Tekhn. Fiz. **2**, 1

15. *Jost A.* (1966) //Berich. Phys. Chem. **70**

16. *Hurwitz P., Kustin K.* (1964) //Inorg. Chem. **3**, 6

17. *Kedrinskii V.K.* (1974) // Arch. Mech. **26**, 3

18. *Berngardt A. R., Kedrinskii V.K., Pal'chikov E.I.* (1995) //Zh. Prikl. Mekh. i Tekh. Fiz. **36**, 2

19. *Kedrinskii V.K.* (1980) //Fiz. Goren. Vzryva **21**, 5

20. *Kedrinskii V.K.* (1997) //J. Shock Waves. **7**, 2

21. *Scarinci T., Bassin X., Lee J., Frost D.* (1992) Propagation of a reactive wave in a bubbly liquid. // In: *Proc. 18th ISSW*, vol 1, ed by K. Takayama (Sendai,1992, SpringerVerlag) pp 481–484

22. *Vshivkov V.A., Kedrinskii V.K., Shokin Yu. I., Dudnikova G.I.* (1998) Shock amplification by bubbly systems with energy release (SABSER).//In: *Proc. 6th Japan–Russian Joint Symposium on Computational Fluid Dynamics* (Nagoya, 1998) pp 58–61

23. *Iordansky S.V.* (1960)// Zh. Prikl. Mekh. i Tekh. Fiz. **1**, 3

24. *Kogarko B.S.* (1961) //Dokl. Akad. Nauk SSSR **137**, 6

25. *Kogarko B.S.* (1964) // Dokl. Akad. Nauk SSSR **155**, 6

26. *Wijngaarden van L.*(1968) // J. Fluid Mech. **33**

27. *Lazareva G.G., Kedrinskii V.K., Shokin Yu.I., Vshivkov V.A., Dudnikova G.I.* 2001 //Dokl. RAN, **381**, 6

28. *Mader Ch., Kedrinskii V.K.* (1987) Accidential detonation in bubbly liquids. // In: *Proc. 16th Intern. Symp. on Shock Tube and Waves* ed by H. Gronig pp 371-376

29. *Todes O.M.* (1933) //J. Phys. Chem. **4**, 1

30. *Taratuta S. P., Kedrinskii V. K., Fomin P. A., Vasiliev A. A.* (1999) Phase transition role in bubble detonation problems. // In: *Proc. 22nd Int. Symp. on Shock Waves* (London, 1999) pp 223–228

31. *Hasegawa T., Fujiwara T.* (1982) Detonation in oxyhydrogen bubbled liquids. // In: *Proc. 19th Intern. Symp. on Combustion* (Haifa, 1982) pp 675–683

32. *Sychev A.I., Pinaev A.V.* (1986) // Zh. Prikl. Mekh. i Tekh. Fiz. **27**, 1

33. *Maslov I.V., Kedrinskii V.K., Taratuta S.P.* (2002) // Journal of Applied Mechanics and Technical Physics **43** 2 101-109

34. *Lazareva G.G., Kedrinskii V.K., Vshivkov V.A.,Dudnikova G.I. , Shokin Yu. I.* (2004) //Zh. Exp. Teor. Fiz. **125**, 5

35. *Makarov A.I., Kedrinskii V.K., Stebnovsky S.V., Takayama K.* (2005) Explosive eruption of volcanos: some approaches to simulation // In: Proceedings of 25ISSW, 17-20 July, 2005, Bangalore, India

36. *Gilbert J.S., Sparks R.S.* (1998) Future research directions on the physics of explosive volcanic eruption. // In: Gilbert J.S., Sparks R.S. (eds) 1998. The physics of explosive volcanic eruption, Geo. Society, London, Special publication, 145, p. 1-7.

37. *Berngardt A.R., Bichenkov E.I., Kedrinskii V.K., Pal'chikov E.I.* (1984) Optic and x-ray investigation of water fracture in rarefaction wave at later Stages // In: Proceedings of IUTAM Symp. on Optical Methods in the Dynamics of Fluids and Solids, Prague, ed. Pichal, p.137-142

38. *Dobran F.* (1992) Nonequilibrium flow in volcanic conduits and application to the eruption of Mt St Helens on May 181980 and Vesuvius in AD79 // J of Volcanology and Geothermal Researches. V.49. p.285-311.

39. *Mader H.* (1998) Conduit flow and fragmentation. // In: Gilbert J.S., Sparks R.S. (eds) 1998. The physics of explosive volcanic eruption, Geological Society, London, Special publication, 145, p. 51-71.